

Research article

Changes of microbial life history strategies to soil nutrient limitations following vegetation restoration and its impact on carbon utilization efficiency



Wenli Zhu^{a,1}, Ming Hao^{a,1}, Wei Zhao^a, Shuhan Yu^a, Zihao Fan^a, Yuchen Liu^a, Xingjian Dun^c, Zixu Zhang^{a,b,*}, Peng Gao^{a,b,**}

^a Mountain Tai Forest Ecosystem Research Station of State Forestry and Grassland Administration, Forestry College, Shandong Agricultural University, Tai'an, Shandong, 271018, China

^b Key Laboratory of Crop Water Physiology and Drought-Tolerance Germplasm Improvement, Ministry of Agriculture and Rural Affairs, College of Agronomy, Shandong Agricultural University, Tai'an, China

^c Shandong Academy of Forestry, Shandong Jinan Urban Ecosystem National Observation and Research Station, Ji'nan, 250014, China

ARTICLE INFO

Keywords:

Soil microbial community
Microbial carbon utilization efficiency
Soil carbon sequestration
Soil C
N and P cycle enzymes

ABSTRACT

Vegetation restoration often leads to changes in soil nutrients, prompting adjustments in microbial growth strategies and compositions. However, how microbial adaptive strategies affect microbial carbon use efficiency (CUE) remains unclear. This study utilized the space-for-time substitution method and involved three forest types in the Taiyi Mountain area as research objects for vegetation restoration: *Platycladus orientalis* (L.) Franco. (PO), *Pinus densiflora* Siebold & Zucc. (PS), and *Quercus acutissima* Carruth. (QA), with shrub (CT) serving as the control. Nutrient limitation changes and microbial adaptation strategies following vegetation restoration were quantified, and microbial CUE was calculated using biogeochemical stoichiometric models to explore how microbial adaptation strategies in response to nutrient limitation changes affect CUE following vegetation restoration. The results revealed that the activities of microbial carbon, nitrogen, and phosphorus cycle enzymes increased to different degrees following vegetation restoration compared with those in the control. Among these, the phosphorus cycle enzyme (ACP) activity in PO and PS increased most significantly, by 26.9 % and 16.8 %, respectively. Following vegetation restoration, compared with CT, the microbial biomass carbon (MBC) of PO increased significantly, from 171.80 µg/g to 382.51 µg/g, and the microbial biomass nitrogen (MBN) of PO also increased significantly, from 19.63 µg/g to 34.91 µg/g. The microbial biomass phosphorus (MBP) decreased significantly, from 11.89 µg/g to 5.52 µg/g. Soil nitrogen limitation was enhanced and shifted from N to P limitation following vegetation restoration. To cope with these limitations, the soil microbial community Chao1 and Shannon decreased significantly, whereas the relative abundance of fungal K-strategy microorganisms increased, indicating a shift in the microbial life history strategy from the r-strategy to the K-strategy. The CUE ranged from 0.39 to 0.49 and significantly increased by 2.5 %, 1.9 %, and 2.4 % for PO, PS, and QA, respectively, following vegetation restoration. Partial least squares modeling (PLS-PM) provided further evidence that moderate nutrient limitation can increase CUE in coniferous forests by altering microbial adaptive strategies. Vegetation restoration induced soil P limitation promotes K-strategy microbes and higher CUE in coniferous forests, potentially making them superior to broadleaf forests for soil carbon sequestration.

* Corresponding author. Mountain Tai Forest Ecosystem Research Station of State Forestry and Grassland Administration, Forestry College, Shandong Agricultural University, Tai'an, Shandong, 271018, China.

** Corresponding author. Mountain Tai Forest Ecosystem Research Station of State Forestry and Grassland Administration, Forestry College, Shandong Agricultural University, Tai'an, Shandong, 271018, China.

E-mail addresses: zhangzx@sda.edu.cn (Z. Zhang), gaopengy@163.com (P. Gao).

¹ Wenli Zhu and Ming Hao contributed equally to this work.

1. Introduction

Vegetation restoration represents a nature-based approach that is widely adopted globally (Bullock et al., 2011; Crouzeilles et al., 2016). The "Bonn Commitment" is the world's first major commitment for forest landscape restoration. It aims to restore 350 million hectares of vegetation by 2030 and has received positive responses from more than 60 countries (Bastin et al., 2019; Parr et al., 2024). According to statistics, the Grain for Green Program (GGP) in 1999 stored 270.8 TgC (Cai et al., 2020; He et al., 2015; Yu et al., 2024). It has been shown that vegetation restoration significantly affects the balance between vegetation and soil carbon, and thus soil organic carbon dynamics, by altering the quantity and quality of apoplastic litter and root secretion (Panchal et al., 2022; Zheng et al., 2024; Zhong et al., 2020). A growing body of research evidence suggests that microbial carbon utilization efficiency (CUE) is a key predictor of soil carbon sequestration capacity (Yuan et al., 2024; Zheng et al., 2024; Yang et al., 2025), and that relatively high CUE indicates that microorganisms take up more organic carbon for their own growth (Fang, 2025; Li et al., 2023; Silva-Sánchez et al., 2019). However, changes in CUE in a global context remain unclear, with some studies suggesting that SOC levels increase with CUE globally (Sinsabaugh et al., 2016; Xiao et al., 2024), but a recent study suggests a negative feedback loop between SOC and CUE (Tan and Luo, 2025). Besides, soil microorganisms play an important catalytic role in this process, with microbial diversity and community structure explaining 36%–50% of CUE variation (Domeignoz-Horta et al., 2020; Pei et al., 2025). How vegetation restoration regulates CUE by altering microbial community characteristics remains poorly understood. Clarifying the effects of vegetation restoration on CUE is essential to exploit the soil carbon sequestration potential of planted forests to realize larger-scale carbon sinks.

As plant growth promotes the gradual transfer of P from mineral soil to aboveground plant biomass, vegetation restoration typically leads to the asynchronous accumulation of soil carbon and nutrients (N and P), which may result in a soil nutrient imbalance (Xu et al., 2021; Yuan et al., 2019). Numerous studies have reported the transformation of and increase in soil nutrient limitation following vegetation restoration, and all of these ecological processes have resulted in an increase in the soil C:N or C:P (Lu et al., 2022; Yan et al., 2022b; Yang et al., 2023a). Notably, the C:N and C:P ratios of forest ecosystem soils are often higher than the actual microbial requirements, which may expose microbial communities in forested lands to unbalanced soil resources and hinder their ability to maintain stable microbial stoichiometry (Du et al., 2024; Yang et al., 2023a). It is now generally accepted that when stoichiometric imbalance occurs, a microbial adaptation strategy at the individual level involving regulating the secretion of extracellular enzymes and adjusting their elemental utilization efficiency leads to a reduction in their CUE (Ju et al., 2024; Yan et al., 2022a). However, its community structure usually also changes to adapt to soil resource conditions under resource-limiting constraints (Cui et al., 2022a; Zhou et al., 2024b). The enormous taxonomic and metabolic diversity of microbes can be simplified by classifying life history strategies. Copiotrophs microbes (r-strategy) grow faster and are more dependent on resource availability, whereas oligotrophic microbes (K-strategy) utilize resources efficiently at the expense of growth rates (Hua et al., 2023; Kaiser et al., 2014; Qin et al., 2025; Zhong et al., 2020). This taxonomy is based primarily on microbial substrate preferences, nutritional strategies, and growth rates and has been widely applied in various environments with good results (Qin et al., 2025; Zhou et al., 2018). However, our understanding of the relationships among nutrient limitations, microbial communities, and CUE following vegetation restoration remains limited. Therefore, it is difficult to fully elucidate the mechanism of action by which vegetation restoration drives soil organic carbon (SOC) pool stabilization and accumulation.

China has 5% of the world's forests, and forest biomass carbon stocks are projected to increase by 13.6 ± 1.5 Pg C by 2100, with C

storage in soils up to 2.1 times higher than that in vegetation (Peng et al., 2016; Sun and Liu, 2019; Yu et al., 2024). In recent decades, China has implemented numerous large-scale vegetation restoration projects. The soils in these restored areas serve as important carbon sinks with significant potential for carbon sequestration (Bell et al., 2023; Cui et al., 2022b). Current research on how vegetation restoration affects CUE is limited and shows conflicting results. Some studies have reported that restoration increases CUE (Li et al., 2023; Yang et al., 2025; Zhong et al., 2020), whereas others have reported that CUE decreases following restoration (Chen et al., 2019; Shi et al., 2024). In addition, many studies have demonstrated differences in soil carbon sequestration mechanisms in different forest stands (especially coniferous and broadleaf forests) (Cotrufo et al., 2013; Xu et al., 2023; Yang et al., 2014; Zheng et al., 2022). According to the growth rate hypothesis, coniferous species generally have lower growth rates than broadleaf species, which results in relatively lower levels of nitrogen and phosphorus in their tissues (Ågren, 2024; Vrede et al., 2004; Zhang et al., 2017). In addition, coniferous forests typically have higher C:N and lower decomposition rates in litter compared to broadleaf forests (Zhang et al., 2017). Coniferous forests put less phosphorus into the soil relative to broadleaf forests and are more likely to contribute to soil phosphorus limitation (Kranabetter et al., 2020; Liu et al., 2023b). Therefore, it was hypothesized that the inconsistent effects of vegetation restoration on CUE may depend on differences in vegetation restoration stands. Nevertheless, evidence regarding how CUE varies across different vegetation restoration conditions remains insufficient.

Therefore, a study was conducted in Yaoxiang National Forest Park in the Taiyi Mountain area. Large-scale vegetation restoration was carried out in this area 40 years ago, including the various vegetation restoration models, which provided a natural platform for the development of this study area. *Platycladus orientalis* (L.) Franco. (PO), *Pinus densiflora* Siebold & Zucc. (PS), *Quercus acutissima* Carruth. (QA), and shrub (CT) were selected as the research objects. Our study applied the Vector-TER model to quantify changes in soil microbial resource constraints. Microbial community characteristics and life history strategies were analyzed through 16S and ITS high-throughput sequencing. CUE was quantified using biogeochemical stoichiometric models. The relationships among microbial resource constraints, community characteristics, life history strategies, and CUE were then examined through partial least squares path analysis (PLS-PM). It was hypothesized that (1) vegetation restoration enhances soil phosphorus limitation and increases the relative abundance of K-strategy microorganisms with greater substrate affinity under limited resources (He et al., 2025). (2) K-strategy microorganisms have greater environmental adaptability under nutrient-limited conditions (Zhong et al., 2020), the CUE of K-strategy microorganisms is higher than that of the r-strategy microorganisms in this environment, and an increase in the relative abundance of K-strategy microorganisms will increase the CUE. (3) Coniferous forests input less P to soil relative to broadleaf forests, resulting in more P limitation (Kranabetter et al., 2020), and the mechanism of CUE enhancement is more pronounced in coniferous forests.

2. Materials and methods

2.1. Sample site overview and experimental design

The study area was located in Yaoxiang National Forest Park in the Taiyi Mountain Area, Tai'an city, Shandong Province, China ($117^{\circ}25'11''E$, $35^{\circ}48'15''N$). The site has a temperate continental semi-humid monsoon climate, with elevations of 310–950 m, an average annual temperature of $18.5^{\circ}C$, and approximately 800 mm of annual precipitation. The shrub layer in the study area was well developed with more than 70% cover, and the dominant species were *Vitex negundo* var. *Heterophylla* (Franch.) Rehd., *Lespedeza bicolor* Turcz., and *Spiraea salicifolia* L. Seasonal water shortages and drought were serious in the study

area. The main established grass species before vegetation restoration were *Themeda triandra* Forssk. and *Setaria viridis* (L.) P. Beauv. Vegetation restoration programs have been started in the last three decades to address environmental challenges, with large areas of pure forest, and significant changes in stand structure and basic soil properties have occurred in the study area following vegetation restoration. The forest stands in the study area are mainly composed of *Platycladus orientalis* (L.) Franco, *Pinus densiflora* Siebold & Zucc., and *Quercus acutissima* Carruth. And the forest understory is less shrubby with the presence of some wattle *Vitex negundo* var. *heterophylla*, significantly altering the forest structure and soil properties (Table 1). The soil type throughout the area is Luvisol. Different stand types maintain similar soil types, stand densities, and altitudes (Table 1).

2.2. Soil sampling and determination of basic physical and chemical properties

The study area included three main forest stands: *Platycladus orientalis* (L.) Franco (PO), *Pinus densiflora* Siebold & Zucc. (PS), and *Quercus acutissima* Carruth. (QA). shrub (CT) was selected as the control and performed three replicates for each stand and control. For each sample, established a 20 × 20 m plot. All plots shared similar geographical features, and maintained a minimum distance of 100 m between neighboring plots. Within each plot, the litter layer were carefully removed and surface cover before sampling, collected the surface (0–10 cm) soil using a systematic five-point sampling method and then homogenized samples from the same soil layer to generate a composite sample. Finally, 12 independent soil samples (4 treatments × 3 replicates) were obtained. A portion of the collected soil was placed in sealed containers and rapidly frozen using dry ice, preserving it for subsequent microbiome analysis through high-throughput DNA sequencing techniques. All soil samples underwent processing to eliminate non-soil components including plant root systems, leaf detritus, and lithic fragments.

Table 1
Plot overview and basic physicochemical properties.

Index	PO	PS	QA	CT
Sand density (stems ha ⁻¹)	17	16	17	975
Soil types	Alfisols	Alfisols	Alfisols	Alfisols
Altitude (m)	567 ± 79a	428 ± 19a	498 ± 26a	486 ± 47a
pH	5.59 ± 0.05b	4.90 ± 0.07c	4.93 ± 0.01c	7.23 ± 0.01a
EC(µS/cm)	34.93 ± 3.12a	30.07 ± 3.16a	26.93 ± 0.12a	30.69 ± 2.75a
SWC(%)	3.68 ± 0.26d	7.59 ± 0.29b	6.67 ± 0.21c	8.74 ± 0.11a
BD(g/cm ³)	1.31 ± 0.02 ab	1.31 ± 0.02 ab	1.45 ± 0.01a	1.22 ± 0.03c
SOC(g/kg)	15.33 ± 0.75a	17.20 ± 1.14a	7.92 ± 0.34b	8.95 ± 0.25b
TN(g/kg)	1.17 ± 0.04a	1.06 ± 0.01b	0.84 ± 0.02c	0.80 ± 0.01c
TP(g/kg)	0.22 ± 0.02a	0.11 ± 0.01b	0.15 ± 0.01b	0.09 ± 0.02b
C:N	13.17 ± 0.56b	16.25 ± 1.07a	9.47 ± 0.44c	11.21 ± 0.23 ab
C:P	72.29 ± 11.12b	163.53 ± 18.49a	54.59 ± 1.72 ab	44.93 ± 4.63 ab
N:P	5.50 ± 0.79b	10.01 ± 0.59a	5.77 ± 0.11b	4.01 ± 0.42b

All values are presented as the mean ± SE. PO: *Platycladus orientalis* (L.) Franco. PS: *Pinus densiflora* Siebold & Zucc. QA: *Quercus acutissima* Carruth. CT:Shrub. SOC: soil organic carbon. TN:total nitrogen. TP:total phosphorus. EC: electrical conductivity. BD: Soil bulk density. C:N: carbon nitrogen ratio.C:P: carbon phosphorus ratio.N:P: nitrogen phosphorus ratio.SWC: soil moisture content. The same letter indicates no significant difference at different vegetation restoration (one-way ANOVA, p < 0.05).

Bulk density (BD) was measured using the cutting ring method, calculated as the dry soil mass divided by the ring volume (Al-Shammary et al., 2018). Soil water content (SWC, %) was determined using the gravimetric approach, baking samples at 105 ± 5 °C until their weight stabilized. For pH analysis, a 1:2.5 soil-water slurry was prepared, and pH was measured with a calibrated pH meter (PHS-3C, INESA, Shanghai Instrument & Electrical Scientific Instrument Co., LTD., China). Soil electrical conductivity (EC, µS/cm) was analyzed via electrode measurement (DDS-307A, INESA, Shanghai Instrument & Electrical Scientific Instrument Co., LTD., China). Organic carbon content (SOC, g/kg) was quantified through Walkley-Black dichromate oxidation (Nelson and Sommers, 1996), while total nitrogen (TN, g/kg) was measured using Kjeldahl digestion (Bremner, 1996). Phosphorus levels (TP, g/kg) were evaluated via molybdenum-antimony colorimetric analysis (Olsen and Sommers, 1982). The microbial carbon (MBC), microbial nitrogen (MBN) and microbial phosphorus (MPB) contents of the soil were determined by chloroform fumigation (Brookes et al., 1985).

2.3. Measurement of soil extracellular enzymes and CUE

The microplate assay quantified five extracellular enzymes linked to C, N, and P cycling (Sinsabaugh et al., 2009; Sinsabaugh and Shah, 2012): β-1,4-Glucosidase (GC) and β-D-cellulosidase (CBH) for the C cycle; β-N-acetylglucosaminopeptidase (NAG) and leucine aminopeptidase (LAP) for the N cycle; and acid phosphatase (AP) for the P cycle. The soil extracellular enzyme stoichiometry was calculated as E_{C:N}=(GC + CBH)/(NAG + LAP), E_{C:P}=(GC + CBH)/AP, and E_{N:P}=(NAG + LAP)/AP. Soil nutrient limitation was assessed via extracellular enzyme stoichiometry using the vector length and angle. The magnitude of the vector length carbon constraints in microbial communities, while vector angle revealed nitrogen and phosphorus limitations. Longer vectors signaled stronger carbon limitation for microorganisms. When vector angle below 45°, nitrogen was the primary limiting factor, whereas angles exceeding 45° pointed to phosphorus constraints (Moorhead et al., 2016).

$$\text{Vector length} = \left\{ \left[\frac{\text{GC} + \text{CBH}}{\text{NAG}} \right]^2 + \left[\frac{\text{BG} + \text{CBH}}{\text{AP}} \right]^2 \right\}^{0.5} \quad (1)$$

$$\text{Vector angle} = \text{Degree} \left\{ \arctan \left[\frac{\text{BG} + \text{CBH}}{\text{AP}}, \frac{\text{BG} + \text{CBH}}{\text{NAG}} \right] \right\} \quad (2)$$

Microbial CUE was assessed using a biogeochemical stoichiometric model (Sinsabaugh and Shah, 2012) with the following formula:

$$\text{CUE} = 0.6 \times \left\{ \frac{\text{S}_{\text{C:N}} \times \text{S}_{\text{C:P}}}{[(0.5 + \text{S}_{\text{C:N}}) \times (0.5 + \text{S}_{\text{C:P}})]} \right\}^{0.5} \quad (3)$$

$$\text{S}_{\text{C:N}} = \frac{\text{Microbial biomass}_{\text{C:N}}}{\text{Soil}_{\text{C:N}}} \times \left(\frac{1}{\text{E}_{\text{C:N}}} \right) \quad (4)$$

$$\text{S}_{\text{C:P}} = \frac{\text{Microbial biomass}_{\text{C:P}}}{\text{Soil}_{\text{C:P}}} \times \left(\frac{1}{\text{E}_{\text{C:P}}} \right) \quad (5)$$

In the formula, the microbial biomass C:N and microbial biomass C:P represent the MBC:MBN and MBC:MPB, respectively. S_{C:N} and S_{C:P} represent the resource availability for microbial growth.

2.4. DNA extraction and microbial gene sequencing

Soil genomic DNA was extracted using a magnetic bead kit (TIANamp Soil DNA Kit, TIANGEN Biotech, Beijing, China) and verified by 1% agarose gel electrophoresis. After PCR amplification, library construction included end repair, A-tailing, adapter ligation, and purification. The bacterial 16S rRNA V3-V4 regions were amplified with the 515F/806R primers, whereas the fungal ITS1 regions were amplified with the ITS5-1737F/ITS2-2043R primers. The fungal primer sequences

in this study were GGAAGTAAAGTCGTAACAAGG and GCTGCCTTCATCGATGC (Chen et al., 2021; Gardes and Bruns, 1993; Liu et al., 2021; White et al., 1990), and the bacterial primer sequences were GTGCCAGCMGCCGCGTAA and GGAC-TACHVGGGTWTCTAAT (Callahan et al., 2016; Caporaso et al., 2011; Chen et al., 2021; Walters et al., 2015; Yang et al., 2023b). Sequencing was conducted using an Illumina NovaSeq 6000. Data processing involved barcode sorting, primer removal, and filtering sequences shorter than 200 bp. Sequences were grouped into ASVs (97 % similarity), taxonomically classified, and normalized to the smallest sample size to minimize depth bias. QIIME 1.9.1 was used to analyze the relative abundance, alpha diversity, and life history strategies of the microbial community.

2.5. Statistical analysis

Bacteria and fungi can be classified by life history strategy at the phylum level. Acidobacteriota, Actinomycetota, and Chloroflexota are oligotrophic (K-strategy) bacteria, whereas Bacteroidota and Gemmatimonadota are copiotrophic (r-strategy). Basidiomycota are oligotrophic (K-strategy) fungi, and Ascomycota are copiotrophic (r-strategy) (Yang et al., 2022; Hua et al., 2023; Li et al., 2021).

Normality and chi-square tests were performed on all data. Shapiro-Wilk test was used for normality test and Levene's test was used for chi-square test with confidence level set at 95 %. One-way ANOVA was performed in SPSS 26.0, followed by Tukey post-hoc tests to compare

differences in microbial diversity indices, life-history strategies, enzyme activities, biomass, stoichiometry, carbon use efficiency (CUE), and nutrient limitation among the PO, PS, QA, and CT treatments. Mantel correlation was used to analyze the relationships of bacterial and fungal community structure and life history strategy with soil extracellular enzyme activity, microbial biomass, and nutrient limitation. A random forest algorithm assessed CUE determinants. Partial least squares path analysis (PLS-PM) was used to verify the impact of the microbial adaptation strategy and changes in the microbial community structure caused by changes in soil resource limitation in coniferous and broad-leaved forests following vegetation restoration on microbial CUE. The production of the correlation graphs was performed using Origin 2024 and the "ggcor," "rfPermute," "ggplot2," and "plspm" packages in R (v4.3.2).

3. Results

3.1. Extracellular enzyme activities and enzyme stoichiometry of soil microorganisms following vegetation restoration

Vegetation restoration had a positive effect on the activities of soil carbon cycle enzymes and nitrogen cycle enzymes. The extracellular enzyme activities of GC, CBH and NAG in PO significantly increased following vegetation restoration compared with the control ($p < 0.05$, Fig. 1a and c). In addition, the extracellular enzyme activities of LAP in PO, PS and QA also significantly increased ($p < 0.05$, Fig. 1b and d). The

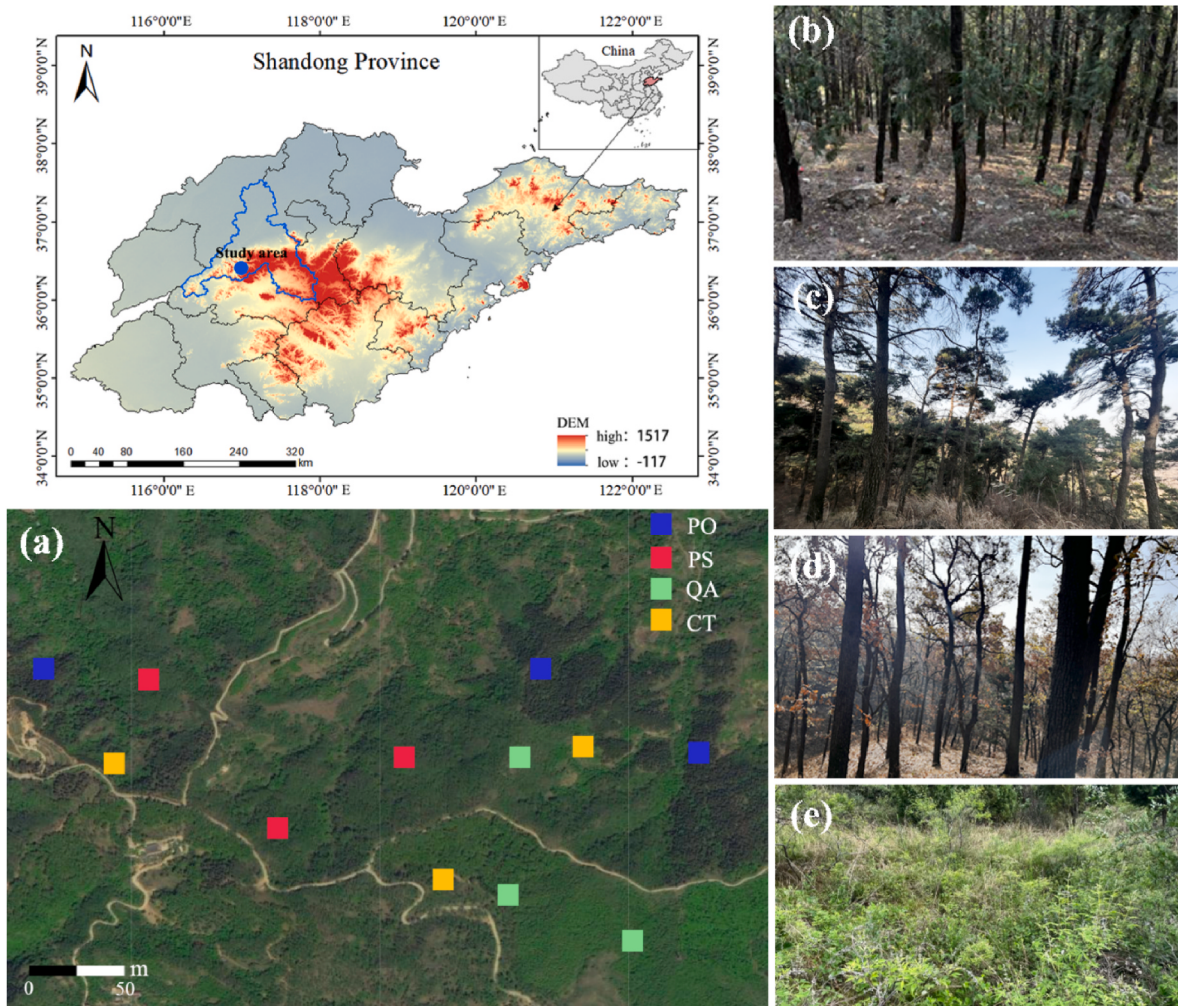


Fig. 1. Regional location and sample site arrangement in the study area. (a) Arrangement of sample sites in the study area (b) *Platycladus orientalis* (L.). Franco., PO. (c) *Pinus densiflora* Siebold & Zucc., PS. (d) *Quercus acutissima* Carruth. QA. (e) Shrub, CT.

activities of soil phosphorus cycling enzymes increased significantly following vegetation restoration, with ACP activities in PO and PS increasing by 26.9 % and 16.8 %, respectively, compared with CT ($p < 0.05$, Fig. 2e). Compared with broad-leaved forests (QA), the activities of carbon cycle enzymes (GC and CBH), nitrogen cycle enzymes (NAG and LAP), and phosphorus cycle enzymes (ACP) in coniferous forests (PO) were significantly increased ($p < 0.05$, Fig. 1a-e). Vegetation restoration changed soil microbial enzyme stoichiometry. In comparison with CT, the $E_{C:P}$ ratio in PS significantly decreased following vegetation restoration ($p < 0.05$, Fig. 2g), while the $E_{N:P}$ ratios in PO and PS also significantly decreased ($p < 0.05$, Fig. 2h). However, the $E_{C:N}$ ratios in PO, PS, and QA did not significantly change ($p > 0.05$, Fig. 2f).

3.2. Soil microbiomass stoichiometry, nutrient limitation and CUE following vegetation restoration

The trends in MBC and MBN contents following vegetation restoration were the same, with significant increases in the MBC and MBN

contents in PO, PS, and QA compared with CT ($p < 0.05$, Table 2). In contrast, the MBP contents in PO, PS, and QA significantly decreased by 5.4 %, 4.7 %, and 5.7 %, respectively, compared CT ($p < 0.05$, Table 2). Compared with QA, the contents of MBC and MBN in PO increased significantly ($p < 0.05$, Table 2), while the content of MBP showed no significant change ($p > 0.05$, Table 2). The trends of the changes in MBC:MBP and MBN:MBP were the same following vegetation restoration ($p < 0.05$, Table 2), and the MBC:MBP and MBN:MBP in PO increased significantly compared with CT ($p < 0.05$, Table 2). The vector angle of QA was 42.99°, indicating significant N limitation in broadleaf forests, while the vector angles of PO and PS were 52.24° and 52.46°, respectively, indicating significant P limitation in coniferous forests. The change in the vector angle from 40.20° (CT) to 52.24° (PO) following vegetation restoration indicated an increase in microbial nutrient limitation and a shift from microbial N limitation to microbial P limitation following vegetation restoration (Fig. 3a and b). The lowest CUE of CT was 0.39, and the highest CUE of PO was 0.49. Compared with that of CT, the CUEs of PO, PS, and QA increased significantly ($p < 0.05$,

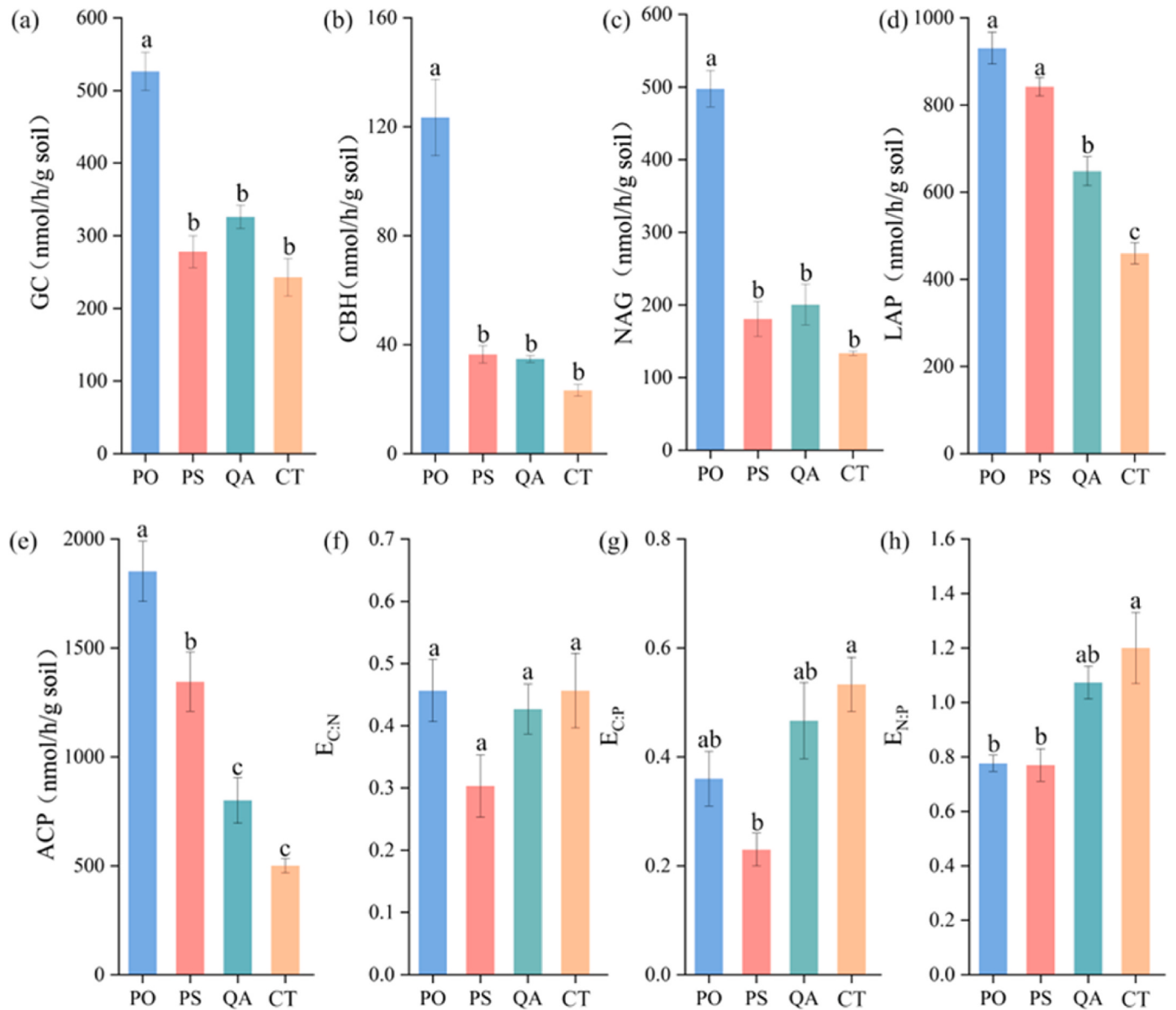


Fig. 2. Soil extracellular enzyme activities(a-d and e) and extracellular enzyme stoichiometry (f-h) following vegetation restoration. PO: *Platycladus orientalis* (L.) Franco. PS: *Pinus densiflora* Siebold & Zucc. QA: *Quercus acutissima* Carruth. CT:Shrub. The same letter indicates no significant difference at different vegetation restoration (one-way ANOVA, $p < 0.05$).

Table 2

Microbial biomass and stoichiometry.

Index	PO	PS	QA	CT
MBC (ug/g)	382.51 ± 10.79a	307.00 ± 32.93 ab	264.98 ± 14.25b	171.80 ± 12.95c
MBN (ug/g)	34.91 ± 3.48a	27.21 ± 1.15 ab	27.54 ± 0.97b	19.63 ± 1.88c
MBP (ug/g)	5.52 ± 1.44b	6.28 ± 1.27b	5.16 ± 0.29b	11.89 ± 0.22a
MBC:MBN	11.12 ± 0.85a	11.22 ± 0.79a	9.63 ± 0.47a	8.80 ± 0.41a
MBC:MBP	78.90 ± 19.39a	50.72 ± 5.08 ab	52.00 ± 6.03 ab	14.45 ± 1.06b
MBN:MBP	7.12 ± 1.82a	4.61 ± 0.68 ab	5.38 ± 0.45 ab	1.65 ± 0.14b

All values are presented as the mean ± SE. PO: *Platycladus orientalis* (L.) Franco. PS: *Pinus densiflora* Siebold & Zucc. QA: *Quercus acutissima* Carruth. CT:Shrub. The same letter indicates no significant difference at different vegetation restoration (one-way ANOVA, $p < 0.05$).

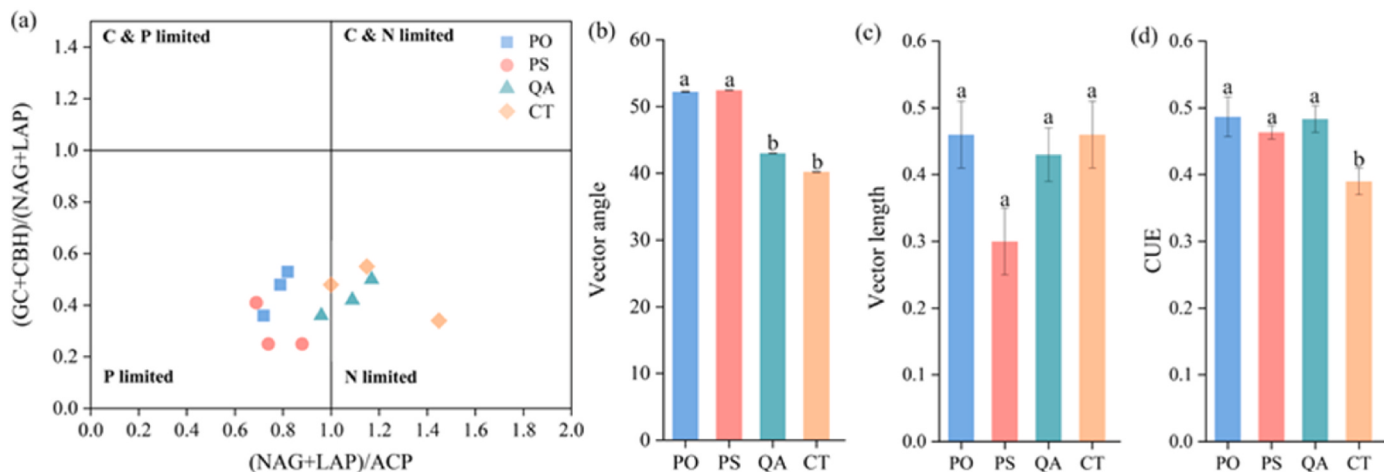


Fig. 3. Soil extracellular enzyme stoichiometry scatter plot (a), nutrient restriction(b,c), and microbial carbon use efficiency(d) following vegetation restoration. Vector length: carbon limited. Vector Angle: Nitrogen limit and phosphorus limit. PO: *Platycladus orientalis* (L.) Franco. PS: *Pinus densiflora* Siebold & Zucc. QA: *Quercus acutissima* Carruth. CT:Shrub. The same letter indicates no significant difference at different vegetation restoration (one-way ANOVA, $p < 0.05$).

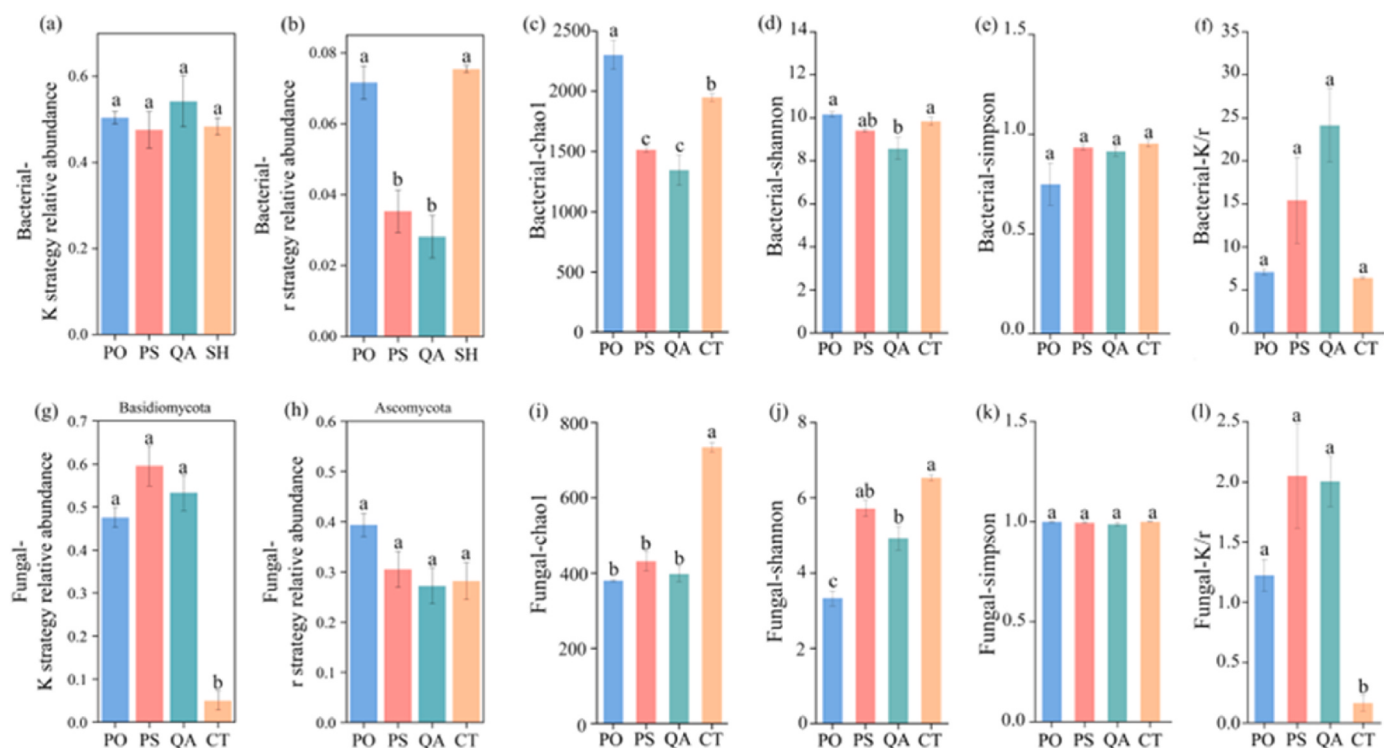


Fig. 4. Relative abundance and community structure of bacterial life history(a-f), Fungal life history relative abundance and community structure(g-l). PO: *Platycladus orientalis* (L.) Franco. PS: *Pinus densiflora* Siebold & Zucc. QA: *Quercus acutissima* Carruth. CT:Shrub. The same letter indicates no significant difference at different vegetation restoration (one-way ANOVA, $p < 0.05$).

Fig. 3d), by 2.5 %, 1.9 %, and 2.4 %, respectively. There was no significant change in CUE for PO and PS compared with QA ($p > 0.05$, **Fig. 3d**). The changes in CUE and microbial nutrient limitation in coniferous forests were more obvious.

3.3. Soil microbial community structure and life history strategy following vegetation restoration

In the bacterial community, the Chao1 indices of PS and QA were significantly lower than CT ($p < 0.05$, **Fig. 4c**), the Chao1 index and Shannon index were significantly higher in PO than in QA ($p < 0.05$, **Fig. 4c** and d). In the fungal community, the Chao1 index and Shannon index of PO and QA were significantly lower than CT ($p < 0.05$, **Fig. 4i** and j). Following vegetation restoration, the proportion of the dominant bacterial phylum gradually increased from 65 % to 78 % (**Table S1**), and the relative abundance of bacterial r-strategy microorganisms in PS and QA decreased significantly ($p < 0.05$, **Fig. 4b**). Compared with CT, the

relative abundances of K-strategy fungi (Basidiomycota) in PO, PS, and QA increased significantly ($p < 0.05$, **Fig. 4g**). Following vegetation restoration, the soil fungal K/r of PO, PS, and QA increased significantly ($p < 0.05$, **Fig. 4l**), indicating that the soil fungal community shifted from the r-strategy to the K-strategy following vegetation restoration (**Fig. 4l**). The bacterial community K/r tended to increase following vegetation restoration, which also indicated that the soil bacterial community shifted from the r-strategy to the K-strategy following vegetation restoration (**Fig. 4f**).

3.4. Relationships among soil microbial nutrient limitation, microbial community structure and CUE following vegetation restoration

The findings of the Mantel analysis indicated that the life history strategy and community structure of fungi following vegetation restoration were extremely significantly correlated with soil pH, LAP, MBC, and MBP ($p < 0.01$) and significantly correlated with ACP and nutrient

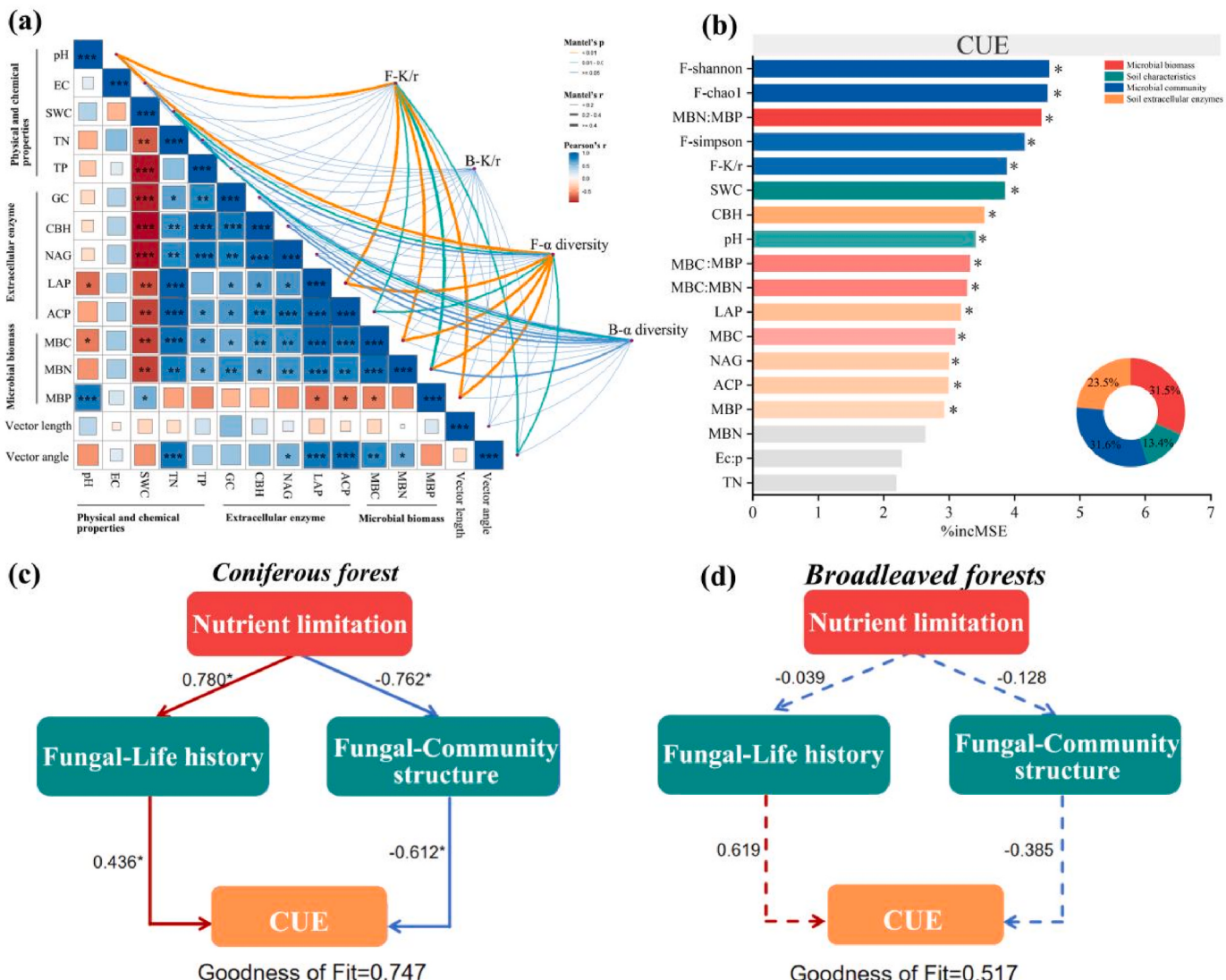


Fig. 5. (a) Mantel analysis showed the correlation of community structure and life history strategy of soil bacteria and fungi with basic soil physicochemical properties, enzyme activities and microbial biomass. (b) Random forest indicates the ranking of importance that influences CUE. (c) Partial least squares path model (PLS-PM) to analyze the effect of nutrient limitation in coniferous forests on the contribution of different pathways to CUE. (d) Partial least squares path model (PLS-PM) to analyze the effect of nutrient limitation in broadleaf forests on the contribution of different pathways to CUE. The value of the indicator is represented by the path coefficient. Positive effects are denoted by red arrows, whereas negative effects are represented by blue arrows. A dashed line signifies that the relationship between the variables is not statistically significant, while a solid line indicates a significant relationship between the variables. CUE: Microbial carbon use efficiency. (*means $p < 0.05$; **means $p < 0.01$; *** means $p < 0.001$).

limitation ($p < 0.05$). In addition, fungal α diversity was significantly correlated with MBN and SWC ($p < 0.05$, Fig. 5a). The life history and community structure of bacteria following vegetation restoration were not significantly correlated with the basic physical and chemical properties of the soil or with microbial nutrient limitations.

The Pearson correlation analysis indicated a significant positive correlation between microbial nutrient limitation following vegetation restoration and both extracellular enzyme activity and microbial biomass ($p < 0.05$, Fig. 5a). The findings derived from the random forest model indicated that the fungal community structure (Shannon, Chao1, Simpson) and K/r strategy had stronger impacts on CUE than did the other factors ($p < 0.05$, Fig. 5b). In addition, MBN:MBP, SWC, pH, and extracellular enzyme activity significantly affected CUE ($p < 0.05$, Fig. 5b). PLS-PM analysis revealed different regulatory mechanisms of CUE following vegetation restoration. In coniferous forests, nutrient limitation significantly affected the fungal life history strategy and community structure ($p < 0.05$, Fig. 5c), thereby regulating CUE. The fungal life history strategy positively affected CUE, whereas the community structure negatively affected CUE (Fig. 5c).

4. Discussion

4.1. Soil phosphorus limitation reshapes soil microbial life history strategies and community structure following vegetation restoration

Vegetation restoration changes the input of soil C, N, and P, thus affecting microbial metabolism, and its extracellular enzyme activity usually changes (Peng and Wang, 2016). Liu et al. (2023a) found that the activities of carbon cycle enzymes (GC and CBH) and nitrogen cycle enzymes (NAG and LAP) of the soil were significantly elevated following vegetation restoration, which was consistent with the results shown in Fig. 2. This is because when stoichiometric imbalance and microbial metabolism were constrained by soil resources following vegetation restoration, microorganisms altered the resource supply by modifying community composition and enhancing extracellular enzyme activity (Xiao et al., 2018; Zhong et al., 2020). These findings aligned with the results presented in Fig. 5a. Phosphorus cycling enzyme activity (ACP) changed significantly following vegetation restoration (Fig. 2e), which may be due to the different P acquisition strategies utilized in different stand types. Specifically, coniferous forests typically increase phosphorus availability directly by increasing phosphorus-cycling enzyme activities (Men et al., 2023). In contrast, broadleaf forests increase organic phosphorus in rhizosphere soil by secreting more low-molecular-weight organic acids (LMWOAs) through their root systems, which stimulates microbial growth and turnover (Li et al., 2022; Mukai et al., 2021; Xia et al., 2020).

Previous research has indicated that phosphorus limitation in soil significantly constrains microbial metabolic processes within forest ecosystems in China (Cui et al., 2022b). The results of the present study showed that vegetation restoration further enhanced the limiting effect of soil phosphorus, a finding that validates existing conclusions (Fig. 3a) and is consistent with hypothesis I. This may be due to the increase in root density following vegetation restoration and the significant increase in plant demand and uptake of phosphorus, which intensifies the competition between plants and microorganisms for phosphorus resources and further deepens microbial limitation of phosphorus (Cui et al., 2022b; Kranabetter et al., 2020; Kuzyakov and Xu, 2013; Philippot et al., 2013). Notably, a shift from nitrogen limitation to phosphorus limitation was observed in the vegetation restoration, in contrast to without vegetation restoration. This transition is likely attributable to the differing nutrient requirements of shrub communities compared to those of other tree communities. Specifically, before vegetation restoration, shrub communities presented more severe soil N limitation, which was likely related to their unique root symbiotic fungal types and nutrient acquisition strategies (Wu et al., 2025). According to the "Gadgil effect," ectomycorrhizal fungi formed symbiotic relationships

with shrubs (Fanin et al., 2022). These mycorrhizal fungi inhibited the activity of free-living saprophytic microorganisms in the soil, thereby slowing litter decomposition and hindering soil nitrogen mineralization processes (Fanin et al., 2022; Sterkenburg et al., 2018; Welker et al., 2024). With the establishment and development of vegetation, increased root exudates and litter inputs significantly increased the soil organic matter content and promoted microbial activity. The improvement in microbial biomass and activity directly strengthened the ability to decompose complex organic nitrogen compounds, facilitating nitrogen mineralization processes (Yang et al., 2021). This finding aligned with our observation of significantly increased nitrogen cycling enzyme activities following vegetation restoration (Fig. 2). Additionally, the increased P demand for plant growth became significant following vegetation restoration. Since soil phosphorus originated primarily from parent material weathering with slow replenishment rates and phosphorus was easily adsorbed and fixed by soil minerals with low bioavailability, phosphorus became a limiting factor (Gao et al., 2019; Yang et al., 2021; Yuan et al., 2019). This ultimately resulted in a transition in soil microbial metabolism from N limitation to P limitation (Soares and Rousk, 2019).

The relative abundance of Basidiomycota, a dominant phylum of K-strategy fungi, increased in the soil following vegetation restoration. The life history strategy of soil microorganisms shifted from the r-strategy to the K-strategy, which supported hypothesis I (Fig. 4j). Similarly, Zhong et al. (2020) clearly showed that stoichiometric imbalances lead to shifts in the life history strategies of major microorganisms. Typically, the r-strategy has higher growth rates and relies on readily available substrates (Yang et al., 2023b; Zhang et al., 2022), but the K-strategy efficiently utilizes stabilizing substrates by lowering growth rates (Pianka, 1970; Shi et al., 2023). Following vegetation restoration, trees input more complex organic compounds (such as lignin and cellulose) into the soil through litter and root exudates (Li et al., 2024). These substances decomposed slowly, and K-strategy microorganisms were typically more effective at utilizing them through extracellular enzyme decomposition (Shi et al., 2023). Consequently, the microbial community evolved to be dominated by the K-strategy following vegetation restoration. This research results revealed that the increased relative abundance of K-strategy microorganisms and the shift in life history strategy following vegetation restoration also supported these findings to some extent (Fig. 4). In addition, the K-strategy fungi were more affected than bacteria following vegetation restoration due to the high dependence of soil fungi on their hosts coupled with the fact that fungi are mainly responsible for cellulose decomposition in forest soils (Santonja et al., 2017; Štúrová et al., 2012). Therefore, the soil fungal communities were more sensitive than bacterial communities to changes in litter composition and diversity caused by changes in aboveground vegetation (Liu et al., 2020; Schütte et al., 2019). Mantel analysis revealed that the fungal life history strategy and community structure were more vulnerable to soil properties than were the bacterial life history strategy and community structure, which also supported these results to some extent (Fig. 5c and d). In addition, the microbial community showed a decline in diversity following vegetation restoration (Fig. 4g and h), which may be related to the fact that all the stands in this study were pure forests. The species richness of pure forest was low, and the composition of understory vegetation was relatively singular, which led to a reduction in root exudates and litter diversity. Numerous studies have indicated that the diversity of root exudates and litter largely determined soil microbial diversity (Gao et al., 2021; Liu et al., 2020), which ultimately led to a decrease in microbial community diversity following vegetation restoration (Huo et al., 2023). Overall, the P limitation induced by vegetation restoration reshaped the soil microbial life history strategy and functions. The microbial community adapted to more complex substrate characteristics and nutrient levels following vegetation restoration by evolving toward K-strategy microorganisms and increasing extracellular enzyme secretion.

4.2. Effects of changes in the microbial adaptation strategy on CUE following vegetation restoration

A meta-analysis of microbial carbon utilization efficiency in different ecosystems revealed that CUE values in forest ecosystems ranged from 0.13 to 0.55 (He et al., 2023). The CUE in this study ranged from 0.39 to 0.49, which was similar to the range reported in previous studies. However, the CUE of the control group was significantly lower than that of the vegetation restoration group, which may have depended on plant community succession. This occurred because differences in species diversity and community composition altered the quantity, quality, and stoichiometric characteristics of organic matter inputs from plants to the soil, which could have cascading effects on microbial metabolic activities (He et al., 2023; Tang et al., 2024). Adequate and high-quality plant inputs (organic matter readily utilized by microorganisms) could promote rapid microbial growth and turnover and increase CUE (Craig et al., 2022; Duan et al., 2023). In contrast, plant biomass and litter inputs tended to be lower in the control group than in the forest group (Table 1), ultimately resulting in a significantly lower CUE in the shrub forests than in the coniferous and broadleaf forests.

Our research results indicated that increased nutrient limitation following vegetation restoration favored increased CUE, which was consistent with hypothesis II (Fig. 3d). The results revealed that soil fungal communities shifted to K-strategy dominance following vegetation restoration (Fig. 4g), and these fungi typically presented relatively high substrate degradation rates due to their ability to synthesize extracellular enzymes. Specifically, K-strategy microorganisms more effectively decomposed complex organic matter (such as lignin and cellulose) and synergistically improved carbon metabolic efficiency through more complex trophic relationships (Laschermes et al., 2016; Shi et al., 2024; Zhong et al., 2020), resulting in a higher CUE (Mooshammer et al., 2014; Soares and Rousk, 2019). Additionally, mycorrhizal type was crucial for CUE, with coniferous forests predominantly forming symbiotic relationships with ectomycorrhizal fungi (Dang et al., 2018). Previous studies have shown significant differences in microbial CUE between arbuscular mycorrhizal-associated trees and ectomycorrhizal-associated trees (Bahram et al., 2020; Yu et al., 2025). Microorganisms associated with ectomycorrhizal soils presented relatively high growth rates, and ectomycorrhizal nonrhizosphere soils presented relatively high CUE (Yu et al., 2025). This could have been one of the reasons for the increased CUE following vegetation restoration.

Interestingly, mechanisms affecting CUE through a microbial adaptation strategy following vegetation restoration were identified in coniferous forests but not in broadleaf forests (Fig. 3d), which was consistent with hypothesis III. This shows that different stands should be studied separately when studying soil CUE changes following vegetation restoration. The mechanisms of CUE changes potentially differed among forest types, possibly due to differences in litter quality. The main carbon source for microbial metabolism was litter (Chen and Hu, 2024; Cui et al., 2024). Broadleaf species produced litter with typically lower C:N ratios and higher quality (easily decomposed and utilized by microorganisms), which resulted in lower microbial metabolic limitations (Li et al., 2020). Additionally, broadleaf forests typically had greater canopy closure and more stable environments, which easily formed microbial communities with more complex network structures. Compared with simpler trophic structures, these multilevel trophic structures generally compensated more effectively for the impacts of nutrient limitations (Xiao et al., 2023; Xu et al., 2023). These factors likely contributed to the differences in the CUE response to vegetation restoration between coniferous and broadleaf forests, suggesting that studying different forest types separately is meaningful when investigating soil CUE changes following vegetation restoration.

Notably, SOC increased significantly in coniferous forests and insignificantly in broadleaf forests following vegetation restoration (Table 1). Vegetation restoration increased CUE through shifts in the

microbial life history strategy, high CUE did not necessarily indicate high carbon sequestration capacity. In particular, K-strategy microorganisms typically had lower growth rates, which might have been unfavorable for converting the abundant carbon sources in forest ecosystems into more stable microbial necromass carbon (Zhou et al., 2024a). This was widely considered to be the reason why soil organic carbon accumulated slowly or did not accumulate in mature forests (Chen et al., 2021; Deng et al., 2022; Shi et al., 2024). Similar patterns have been observed in other studies. Ji et al. (2017) noted that long-term growth in broadleaf forests after premature stand age no longer favors soil C accumulation and may promote surface soil C loss. However, a higher CUE indicated more efficient C metabolism, which helped maintain existing soil carbon levels. Additionally, the three vegetation restoration types selected in this study were all pure forests, which ensured consistency of effects but somewhat neglected mixing effects. More diverse carbon sources in mixed forests could, to some extent, help avoid nutrient limitations for soil microorganisms. Therefore, future meta-analytic studies of nutrient limitation and CUE following vegetation restoration are encouraged to consider both forest types and mixed forest effects.

5. Conclusion

These findings support our hypotheses, confirming that vegetation restoration enhances soil phosphorus limitation, promotes the dominance of K-strategy microorganisms with greater substrate affinity, and increases microbial carbon use efficiency under nutrient-limited conditions. Furthermore, the before mentioned mechanisms were observed only in coniferous forest vegetation restoration, possibly due to differences in litter properties and microclimate between coniferous and broadleaf forests. Although increased CUE alone did not represent increased soil carbon sequestration capacity, the improvement in CUE following vegetation restoration indicated that it at least helped maintain existing soil carbon levels. To better achieve carbon sequestration, introducing coniferous species during the transformation of broadleaved forests is recommended, given the greater soil carbon storage potential of coniferous forests. These findings provide practical guidance for optimizing vegetation restoration and forest management strategies, offering insights into the mechanisms through which vegetation restoration promotes soil organic carbon sequestration and accumulation. It also helps to elucidate the influence of vegetation restoration in coniferous and broad-leaved forests on soil carbon dynamics, which in turn provides innovative research perspectives for revealing the soil carbon cycle process of vegetation restoration in different forest types.

CRediT authorship contribution statement

Wenli Zhu: Writing – original draft, Visualization, Software, Investigation, Formal analysis, Data curation, Conceptualization. **Ming Hao:** Visualization, Validation, Supervision, Software, Data curation. **Wei Zhao:** Supervision, Software, Data curation. **Shuhan Yu:** Visualization, Supervision, Data curation. **Zihao Fan:** Validation, Supervision. **Yuchen Liu:** Validation, Supervision, Data curation. **Xingjian Dun:** Supervision, Project administration, Investigation. **Zixu Zhang:** Writing – review & editing, Validation, Supervision, Resources, Methodology, Investigation, Funding acquisition. **Peng Gao:** Writing – review & editing, Validation, Supervision, Resources, Methodology, Funding acquisition, Formal analysis.

Declaration of competing interest

The authors declare that they have no known competing financial interests or personal relationships that could have appeared to influence the work reported in this paper.

Acknowledgments

This research was financially supported by the National Key Research and Development Program of China (grant No. 2024YFD2200500); the Central Financial Forestry Science and Technology Promotion Demonstration Project (Grant number LU [2023] TG008); the National Natural Science Foundation of China(42207373); Program for Scientific Research Innovation Team of Young Scholar in Colleges and Universities of Shandong Province (2024KJG043); Shandong Provincial "811" Project of First-class Discipline Construction.

Appendix A. Supplementary data

Supplementary data to this article can be found online at <https://doi.org/10.1016/j.jenvman.2025.126684>.

Data availability

The authors do not have permission to share data.

References

- Ågren, G.I., 2024. Plant stoichiometry in relation to relative growth rate. *J. Plant Ecol.* 17, 1–6. <https://doi.org/10.1093/jpe/rtae095>.
- Al-Shammary, A.A.G., Kouzani, A.Z., Kaynak, A., Khoo, S.Y., et al., 2018. Soil bulk density estimation methods: a review. *Pedosphere* 28, 581–596. [https://doi.org/10.1016/S1002-0160\(18\)60034-7](https://doi.org/10.1016/S1002-0160(18)60034-7).
- Bahram, M., Netherway, T., Hildebrand, F., Pritsch, K., et al., 2020. Plant nutrient-acquisition strategies drive topsoil microbiome structure and function. *New Phytol.* 227, 1189–1199. <https://doi.org/10.1111/nph.16598>.
- Bastin, J.-F., Finegold, Y., Garcia, C., Mollicone, D., et al., 2019. The global tree restoration potential. *Science* 365, 76–79. <https://doi.org/10.1126/science.aax0848>.
- Bell, S.M., Raymond, S.J., Yin, H., Jiao, W., et al., 2023. Quantifying the recarbonization of post-agricultural landscapes. *Nat. Commun.* 14, 2139. <https://doi.org/10.1038/s41467-023-37907-w>.
- Bullock, J.M., Aronson, J., Newton, A.C., Pywell, R.F., Rey-Benayas, J.M., 2011. Restoration of ecosystem services and biodiversity: conflicts and opportunities. *Trends Ecol. Evol.* 26, 541–549. <https://doi.org/10.1016/j.tree.2011.06.011>.
- Bremner, J.M., 1996. Nitrogen-total. *Methods of soil analysis: Part 3 Chemical methods*, 5, 1085–1121.
- Brookes, P.C., Landman, A., Pruden, G., Jenkinson, D.S., 1985. Chloroform fumigation and the release of soil nitrogen: a rapid direct extraction method to measure microbial biomass nitrogen in soil. *Soil Biol. Biochem.* 17, 837–842. [https://doi.org/10.1016/0038-0717\(85\)90144-0](https://doi.org/10.1016/0038-0717(85)90144-0).
- Cai, D., Ge, Q., Wang, X., Liu, B., et al., 2020. Contributions of ecological programs to vegetation restoration in arid and semiarid China. *Environ. Res. Lett.* 15, 114046. <https://doi.org/10.1088/1748-9326/abde9>.
- Callahan, B.J., McMurdie, P.J., Rosen, M.J., Han, A.W., et al., 2016. DADA2: high-resolution sample inference from Illumina amplicon data. *Nat. Methods* 13, 581–583. <https://doi.org/10.1038/nmeth.3869>.
- Caporaso, J.G., Lauber, C.L., Walters, W.A., Berg-Lyons, D., et al., 2011. Global patterns of 16S rRNA diversity at a depth of millions of sequences per sample. *Proc. Natl. Acad. Sci.* 108, 4516–4522. <https://doi.org/10.1073/pnas.1000080107>.
- Chen, Y., Neilson, J.W., Kushwaha, P., Maier, R.M., Barberán, A., 2021. Life-history strategies of soil microbial communities in an arid ecosystem. *ISME J.* 15, 649–657. <https://doi.org/10.1038/s41396-020-00803-y>.
- Crouzelles, R., Curran, M., Ferreira, M.S., Lindenmayer, D.B., et al., 2016. A global meta-analysis on the ecological drivers of forest restoration success. *Nat. Commun.* 7, 11666. <https://doi.org/10.1038/ncomms11666>.
- Chen, Y., Hu, H.-W., 2024. Impacts of tree species diversity on microbial carbon use efficiency. *Glob. Change Biol.* 30, e17015. <https://doi.org/10.1111/gcb.17015>.
- Chen, Z., Shen, Y., Tan, B., Li, H., et al., 2021. Decreased soil organic carbon under litter input in three subalpine forests. *Forests* 12, 1479. <https://doi.org/10.3390/f12111479>.
- Chen, Z., Yu, G., Wang, Q., 2019. Magnitude, pattern and controls of carbon flux and carbon use efficiency in China's typical forests. *Global Planet. Change* 172, 464–473. <https://doi.org/10.1016/j.gloplacha.2018.11.004>.
- Cotrufo, M.F., Wallenstein, M.D., Boot, C.M., Denef, K., Paul, E., 2013. The Microbial Efficiency-Matrix Stabilization (MEMS) framework integrates plant litter decomposition with soil organic matter stabilization: do labile plant inputs form stable soil organic matter? *Glob. Change Biol.* 19, 988–995. <https://doi.org/10.1111/gcb.12113>.
- Craig, M.E., Geyer, K.M., Beidler, K.V., Brzostek, E.R., et al., 2022. Fast-decaying plant litter enhances soil carbon in temperate forests but not through microbial physiological traits. *Nat. Commun.* 13, 1229. <https://doi.org/10.1038/s41467-022-287159>.
- Cui, J., Zhang, S., Wang, X., Xu, X., et al., 2022a. Enzymatic stoichiometry reveals phosphorus limitation-induced changes in the soil bacterial communities and element cycling: evidence from a long-term field experiment. *Geoderma* 426, 116124. <https://doi.org/10.1016/j.geoderma.2022.116124>.
- Cui, Y., Bing, H., Moorhead, D.L., Delgado-Baquerizo, M., et al., 2022b. Ecoenzymatic stoichiometry reveals widespread soil phosphorus limitation to microbial metabolism across Chinese forests. *Commun. Earth Environ.* 3. <https://doi.org/10.1038/s43247-022-005235>.
- Cui, Y., Hu, J., Peng, S., Delgado-Baquerizo, M., et al., 2024. Limiting resources define the global pattern of soil microbial carbon use efficiency. *Adv. Sci.* 11, 2308176. <https://doi.org/10.1002/advs.202308176>.
- Dang, P., Vu, N.H., Shen, Z., Liu, J., et al., 2018. Changes in soil fungal communities and vegetation following afforestation with *Pinus tabulaeformis* on the Loess Plateau. *Ecosphere* 9. <https://doi.org/10.1002/ecs.2.2401>.
- Deng, W., Wang, X., Hu, H., Zhu, M., et al., 2022. Variation characteristics of soil organic carbon storage and fractions with stand age in north subtropical *Quercus acutissima* Carruth Forest in China. *Forests* 13, 1649. <https://doi.org/10.3390/f13101649>.
- Domeignoz-Horta, L.A., Pold, G., Liu, X.-J.A., Frey, S.D., et al., 2020. Microbial diversity drives carbon use efficiency in a model soil. *Nat. Commun.* 11, 3684. <https://doi.org/10.1038/s41467-020-17502z>.
- Du, Y., Wei, Y., Zhou, Y., Wang, Y., et al., 2024. Temporal variation of microbial nutrient limitation in citrus plantations: insights from soil enzyme stoichiometry. *Environ. Res.* 258, 119275. <https://doi.org/10.1016/j.envres.2024.119275>.
- Duan, P., Fu, R., Nottingham, A.T., Domeignoz-Horta, L.A., et al., 2023. Tree species diversity increases soil microbial carbon use efficiency in a subtropical forest. *Glob. Change Biol.* 29, 7131–7144. <https://doi.org/10.1111/gcb.16971>.
- Fang, L., 2025. Multifaceted links between microbial carbon use efficiency and soil organic carbon sequestration. *Glob Chang Biol* 31, e70045. <https://doi.org/10.1111/gcb.70045>.
- Fanin, N., Clemmensen, K.E., Lindahl, B.D., Farrell, M., et al., 2022. Ericoid shrubs shape fungal communities and suppress organic matter decomposition in boreal forests. *New Phytol.* 236, 684–697. <https://doi.org/10.1111/nph.18353>.
- Gardes, M., Bruns, T.D., 1993. ITS primers with enhanced specificity for basidiomycetes - application to the identification of mycorrhizae and rusts. *Mol. Ecol.* 2, 113–118. <https://doi.org/10.1111/j.1365-294X.1993.tb00005.x>.
- Gao, X.-L., Li, X.G., Zhao, L., Kuzyakov, Y., 2019. Regulation of soil phosphorus cycling in grasslands by shrubs. *Soil Biol. Biochem.* 133, 1–11. <https://doi.org/10.1016/j.soilbio.2019.02.012>.
- Gao, Y., Wang, X., Mao, Z., Yang, L., et al., 2021. Changes in soil microbial community structure following different tree species functional traits afforestation. *Forests* 12, 1018.
- He, B., Miao, L., Cui, X., Wu, Z., 2015. Carbon sequestration from China's afforestation projects. *Environ. Earth Sci.* 74, 5491–5499. <https://doi.org/10.1007/s12665-015-4559-4>.
- He, D., Dai, Z., Cheng, S., Shen, H., et al., 2025. Microbial life-history strategies and genomic traits between pristine and cropland soils. *mSystems* 10, e0017825. <https://doi.org/10.1128/msystems.00178-25>.
- He, P., Zhang, Y., Shen, Q., Ling, N., Nan, Z., 2023. Microbial carbon use efficiency in different ecosystems: a meta-analysis based on a biogeochemical equilibrium model. *Glob. Change Biol.* 29, 4758–4774. <https://doi.org/10.1111/gcb.16861>.
- Hua, P.L., Zhang, W., Kuzyakov, Y., Xiao, L.M., et al., 2023. Linking bacterial life strategies with soil organic matter accrual by karst vegetation restoration. *Soil Biol. Biochem.* 177. <https://doi.org/10.1016/j.soilbio.2022.108925>.
- Huo, X., Ren, C., Wang, D., Wu, R., et al., 2023. Microbial community assembly and its influencing factors of secondary forests in Qinling Mountains. *Soil Biol. Biochem.* 184, 109075. <https://doi.org/10.1016/j.soilbio.2023.109075>.
- Ji, Y.-h., Guo, K., Fang, S.-b., Xu, X.-n., et al., 2017. Long-term growth of temperate broadleaved forests no longer benefits soil C accumulation. *Sci. Rep.* 7, 42328. <https://doi.org/10.1038/srep42328>.
- Ju, W., Sardans, J., Bing, H., Wang, J., et al., 2024. Diversified vegetation cover alleviates microbial resource limitations within soil aggregates in tailings. *Environmental Science & Technology* 58, 18744–18755. <https://doi.org/10.1021/acs.est.4c06081>.
- Kaiser, C., Franklin, O., Dieckmann, U., Richter, A., 2014. Microbial community dynamics alleviate stoichiometric constraints during litter decay. *Ecol. Lett.* 17, 680–690. <https://doi.org/10.1111/ele.12269>.
- Kranabetter, J.M., Sholinder, A., de Montigny, L., 2020. Contrasting conifer species productivity in relation to soil carbon, nitrogen and phosphorus stoichiometry of British Columbia's perhumid rainforests. *Biogeosciences* 17, 1247–1260. <https://doi.org/10.5194/bg-17-1247-2020>.
- Kuzyakov, Y., Xu, X., 2013. Competition between roots and microorganisms for nitrogen: mechanisms and ecological relevance. *New Phytol.* 198, 656–669. <https://doi.org/10.1111/nph.12235>.
- Lashermes, G., Gaynors-Claisse, A., Recous, S., Bertrand, I., 2016. Enzymatic strategies and carbon use efficiency of a litter-decomposing fungus grown on maize leaves, stems, and roots. *Front. Microbiol.* 7, 1315. <https://doi.org/10.3389/fmicb.2016.01315>.
- Li, H., Yang, S., Semenov, M.V., Yao, F., et al., 2021. Temperature sensitivity of SOM decomposition is linked with a K-selected microbial community. *Glob. Change Biol.* 27, 2763–2779. <https://doi.org/10.1111/gcb.15593>.
- Li, J., Dong, L., Fan, M., Shangguan, Z., 2024. Long-term vegetation restoration promotes lignin phenol preservation and microbial anabolism in forest plantations: implications for soil organic carbon dynamics. *Sci. Total Environ.* 928, 172635. <https://doi.org/10.1016/j.scitotenv.2024.172635>.
- Li, Q., Jia, W., Wu, J., Wang, L., et al., 2023. Changes in soil organic carbon stability in association with microbial carbon use efficiency following 40 years of afforestation. *Catena* 228, 10719. <https://doi.org/10.1016/j.catena.2023.10719>.
- Li, Q., Zhang, M., Geng, Q., Jin, C., et al., 2020. The roles of initial litter traits in regulating litter decomposition: a "common plot" experiment in a subtropical

- evergreen broadleaf forest. *Plant Soil* 452, 207–216. <https://doi.org/10.1007/s11104-020-04563-8>.
- Li, Y., Sun, L., Zhu, B., 2022. Trade-offs among fine-root phosphorus-acquisition strategies of 15 tropical woody species. *Forest Ecosystems* 9, 100055. <https://doi.org/10.1016/j.fecs.2022.100055>.
- Liú, G., Wang, H., Yan, G., Wang, M., et al., 2023a. Soil enzyme activities and microbial nutrient limitation during the secondary succession of boreal forests. *Catena* 230, 107268. <https://doi.org/10.1016/j.catena.2023.107268>.
- Liú, J., Fang, L., Qiu, T., Bing, H., et al., 2023b. Disconnection between plant-microbial nutrient limitation across forest biomes. *Funct. Ecol.* 37, 2271–2281. <https://doi.org/10.1111/1365-2435.14361>.
- Liu, J., Le, T. h., Zhu, H., Yao, Y., et al., 2020. Afforestation of cropland fundamentally alters the soil fungal community. *Plant Soil* 457, 279–292. <https://doi.org/10.1007/s11104-020-04739-2>.
- Liu, Y., Wang, H., Peng, Z., Li, D., et al., 2021. Regulation of root secondary metabolites by partial root-associated microbiotas under the shaping of licorice ecotypic differentiation in northwest China. *J. Integr. Plant Biol.* 63, 2093–2109. <https://doi.org/10.1111/jipb.13179>.
- Lu, Z.-X., Wang, P., Ou, H.-B., Wei, S.-X., et al., 2022. Effects of different vegetation restoration on soil nutrients, enzyme activities, and microbial communities in degraded karst landscapes in southwest China. *For. Ecol. Manag.* 508, <https://doi.org/10.1016/j.foreco.2021.120002>.
- Men, X., Bao, Y., Wu, M., Liao, C., Cheng, X., 2023. Soil enzyme activities responded differently to short-term litter input manipulation under coniferous and broad-leaved forests in the subalpine area of Southwest China. *For. Ecol. Manag.* 546, 121360. <https://doi.org/10.1016/j.foreco.2023.121360>.
- Moorhead, D.L., Sinsabaugh, R.L., Hill, B.H., Weintraub, M.N., 2016. Vector analysis of ecoenzyme activities reveal constraints on coupled C, N and P dynamics. *Soil Biol. Biochem.* 93, 1–7. <https://doi.org/10.1016/j.soilbio.2015.10.019>.
- Mooshammer, M., Wanek, W., Zechmeister-Boltenstern, S., Richter, A.A., 2014. Stoichiometric imbalances between terrestrial decomposer communities and their resources: mechanisms and implications of microbial adaptations to their resources. *Front. Microbiol.* 5.
- Mukai, M., Aiba, S-i., Kitayama, K., 2021. Effects of tree-root exudates on the solubilization of phosphorus adsorbed to non-crystalline minerals in the rhizosphere volcanic soils on Yakushima Island, Japan. *Trees (Berl.)* 35, 2031–2041. <https://doi.org/10.1007/s00468-021-02170-3>.
- Nelson, D.W., Sommers, L.E., 1996. Total Carbon, Organic Carbon, and Organic Matter, Methods of Soil Analysis, pp. 961–1010.
- Olsen, S.R., Sommers, L.E., 1982. Phosphorus, Methods of Soil Analysis, pp. 403–430.
- Parr, C.L., te Beest, M., Stevens, N., 2024. Confusion of reforestation with restoration is widespread. *Science* 383, 698–701. <https://doi.org/10.1126/science.adj0899>.
- Panchal, P., Preece, C., Peñuelas, J., Giri, J., 2022. Soil carbon sequestration by root exudates. *Trends Plant Sci.* 27, 749–757. <https://doi.org/10.1016/j.tplants.2022.04.009>.
- Pei, J., Li, J., Luo, Y., Rillig, M.C., et al., 2025. Patterns and drivers of soil microbial carbon use efficiency across soil depths in forest ecosystems. *Nat. Commun.* 16, 5218. <https://doi.org/10.1038/s41467-025-605948>.
- Peng, S., Wen, D., He, N., Yu, G., et al., 2016. Carbon storage in China's forest ecosystems: estimation by different integrative methods. *Ecol. Evol.* 6, 3129–3145. <https://doi.org/10.1002/eece3.2114>.
- Peng, X., Wang, W., 2016. Stoichiometry of soil extracellular enzyme activity along a climatic transect in temperate grasslands of northern China. *Soil Biol. Biochem.* 98, 74–84. <https://doi.org/10.1016/j.soilbio.2016.04.008>.
- Philipott, L., Raaijmakers, J.M., Lemanceau, P., van der Putten, W.H., 2013. Going back to the roots: the microbial ecology of the rhizosphere. *Nat. Rev. Microbiol.* 11, 789–799. <https://doi.org/10.1038/nrmicro3109>.
- Pianka, E.R., 1970. On r- and K-Selection. *Am. Nat.* 104, 592–597. <https://doi.org/10.1086/282697>.
- Qin, Q., Wang, Y., Liu, Y., 2025. Forest wildfire increases the seasonal allocation of soil labile carbon fractions due to the transition from microbial K- to r-strategists. *Environmental Science & Technology* 59, 3537–3547. <https://doi.org/10.1021/acs.est.4c07470>.
- Santonja, M., Rancon, A., Fromin, N., Baldy, V., et al., 2017. Plant litter diversity increases microbial abundance, fungal diversity, and carbon and nitrogen cycling in a Mediterranean shrubland. *Soil Biol. Biochem.* 111, 124–134. <https://doi.org/10.1016/j.soilbio.2017.04.006>.
- Schütte, U.M.E., Henning, J.A., Ye, Y., Bowling, A., et al., 2019. Effect of permafrost thaw on plant and soil fungal community in a boreal forest: does fungal community change mediate plant productivity response? *J. Ecol.* 107, 1737–1752. <https://doi.org/10.1111/1365-2745.13139>.
- Shi, J., Deng, L., Wu, J., Bai, E., et al., 2024. Soil organic carbon increases with decreasing microbial carbon use efficiency during vegetation restoration. *Glob. Change Biol.* 30, e17616. <https://doi.org/10.1111/gcb.17616>.
- Shi, J., Yang, L., Liao, Y., Li, J., et al., 2023. Soil labile organic carbon fractions mediate microbial community assembly processes during long-term vegetation succession in a semiarid region. *iMeta* 2, e142. <https://doi.org/10.1002/imt.2.142>.
- Silva-Sánchez, A., Soares, M., Rousk, J., 2019. Testing the dependence of microbial growth and carbon use efficiency on nitrogen availability, pH, and organic matter quality. *Soil Biol. Biochem.* 134, 25–35. <https://doi.org/10.1016/j.soilbio.2019.03.008>.
- Sinsabaugh, R.L., Hill, B.H., Follstad Shah, J.J., 2009. Ecoenzymatic stoichiometry of microbial organic nutrient acquisition in soil and sediment. *Nature* 462, 795–798. <https://doi.org/10.1038/nature08632>.
- Sinsabaugh, R.L., Turner, B.L., Talbot, J.M., Waring, B.G., et al., 2016. Stoichiometry of microbial carbon use efficiency in soils. *Ecol. Monogr.* 86, 172–189. <https://doi.org/10.1890/15-2110.1>.
- Sinsabaugh, R.L., Shah, J.J.F., 2012. Ecoenzymatic stoichiometry and ecological theory. In: Futuyma, D.J. (Ed.), Annual Review of Ecology, Evolution, and Systematics, vol. 43, pp. 313–343.
- Soares, M., Rousk, J., 2019. Microbial growth and carbon use efficiency in soil: links to fungal-bacterial dominance, SOC-quality and stoichiometry. *Soil Biol. Biochem.* 131, 195–205. <https://doi.org/10.1016/j.soilbio.2019.01.010>.
- Sterkenburg, E., Clemmensen, K.E., Ekblad, A., Finlay, R.D., Lindahl, B.D., 2018. Contrasting effects of ectomycorrhizal fungi on early and late stage decomposition in a boreal forest. *ISME J.* 12, 2187–2197. <https://doi.org/10.1038/s41396-018-0181-2>.
- Štursová, M., Žifčáková, L., Leigh, M.B., Burgess, R., Baldrian, P., 2012. Cellulose utilization in forest litter and soil: identification of bacterial and fungal decomposers. *FEMS (Fed. Eur. Microbiol. Soc.) Microbiol. Ecol.* 80, 735–746. <https://doi.org/10.1111/j.1574-6941.2012.01343.x>.
- Sun, W., Liu, X., 2019. Review on carbon storage estimation of forest ecosystem and applications in China. *Forest Ecosystems* 7, 4. <https://doi.org/10.1186/s40663-019-02102>.
- Tan, B., Luo, S., 2025. Microbial carbon use efficiency and soil organic carbon: which is the determinant? *Innovation*, 100984. <https://doi.org/10.1016/j.inn.2025.100984>.
- Tang, X., Li, Z., Yuan, J., Yu, W., Luo, W., 2024. Biotic and abiotic factors affecting soil microbial carbon use efficiency. *Front. Plant Sci.* 15.
- Vrede, T., Dobberfuhl, D.R., Kooijman, S.A.L.M., Elser, J.J., 2004. Fundamental connections among organism C:N:P stoichiometry, macromolecular composition, and growth. *Ecology* 85, 1217–1229. <https://doi.org/10.1890/02-0249>.
- Walters, W., Hyde Embretson, R., Berg-Lyons, D., Ackermann, G., et al., 2015. Improved bacterial 16S rRNA gene (V4 and V4-5) and fungal internal transcribed spacer marker gene primers for microbial community surveys. *mSystems* 1. <https://doi.org/10.1128/msystems.00009-15>.
- Welker, L., Ward, E.B., Bradford, M.A., Ferraro, K.M., 2024. Plant functional type shapes nitrogen availability in a regenerating forest. *Plant Soil* 499, 587–603. <https://doi.org/10.1007/s11104-024-06483-3>.
- White, T.J., Bruns, T., Lee, S., Taylor, J., 1990. 38 - amplification and direct sequencing of fungal ribosomal rna genes for phylogenetics. In: Innis, M.A., Gelfand, D.H., Sninsky, J.J., White, T.J. (Eds.), PCR Protocols. Academic Press, San Diego, pp. 313–322.
- Wu, X., Liang, Y., Zhao, W., Pan, F., 2025. Root and mycorrhizal nutrient acquisition strategies in the succession of subtropical forests under N and P limitation. *BMC Plant Biol.* 25, 8. <https://doi.org/10.1186/s12870-024-060161>.
- Xia, Z., He, Y., Yu, L., Lv, R., et al., 2020. Sex-specific strategies of phosphorus (P) acquisition in *Populus cathayana* as affected by soil P availability and distribution. *New Phytol.* 225, 782–792. <https://doi.org/10.1111/nph.16170>.
- Xiao, H., Sheng, H., Zhang, L., Zhang, L., et al., 2023. How does land-use change alter soil microbial diversity, composition, and network in subtropical China? *Catena* 231, 107335. <https://doi.org/10.1016/j.catena.2023.107335>.
- Xiao, K.-Q., Liang, C., Wang, Z., Peng, J., et al., 2024. Beyond microbial carbon use efficiency. *Natl. Sci. Rev.* 11, nwae059. <https://doi.org/10.1093/nsr/nwae059>.
- Xiao, W., Chen, X., Jing, X., Zhu, B., 2018. A meta-analysis of soil extracellular enzyme activities in response to global change. *Soil Biol. Biochem.* 123, 21–32. <https://doi.org/10.1016/j.soilbio.2018.05.001>.
- Xu, M., Jian, J., Wang, J., Zhang, Z., et al., 2021. Response of root nutrient resorption strategies to rhizosphere soil microbial nutrient utilization along *Robinia pseudoacacia* plantation chronosequence. *For. Ecol. Manag.* 489, 119053. <https://doi.org/10.1016/j.foreco.2021.119053>.
- Xu, Z., Hu, Z., Jiao, S., Bell, S.M., et al., 2023. Depth-dependent effects of tree species identity on soil microbial community characteristics and multifunctionality. *Sci. Total Environ.* 878, 162972. <https://doi.org/10.1016/j.scitotenv.2023.162972>.
- Yan, B., Duan, M., Wang, R., Li, J., et al., 2022a. Planted forests intensified soil microbial metabolic nitrogen and phosphorus limitation on the Loess Plateau, China. *Catena* 211. <https://doi.org/10.1016/j.catena.2021.105982>.
- Yan, B., Duan, M., Wang, R., Li, J., et al., 2022b. Planted forests intensified soil microbial metabolic nitrogen and phosphorus limitation on the Loess Plateau, China. *Catena* 211, 105982. <https://doi.org/10.1016/j.catena.2021.105982>.
- Yang, J., Wang, Z., Chang, Q., Liu, Z., et al., 2025. Temperature effects on microbial carbon use efficiency and priming effects in soils under vegetation restoration. *Catena* 249, 108632. <https://doi.org/10.1016/j.catena.2024.108632>.
- Yang, S., Feng, C., Ma, Y., Wang, W., et al., 2021. Transition from N to P limited soil nutrients over time since restoration in degraded subtropical broadleaved mixed forests. *For. Ecol. Manag.* 494, 119298. <https://doi.org/10.1016/j.foreco.2021.119298>.
- Yang, S., Wu, H., Wang, Z.R., Semenov, M.V., et al., 2022. Linkages between the temperature sensitivity of soil respiration and microbial life strategy are dependent on sampling season. *Soil Biol. Biochem.* 172. <https://doi.org/10.1016/j.soilbio.2022.108758>.
- Yang, T., Zhang, H., Zheng, C., Wu, X., et al., 2023a. Bacteria life-history strategies and the linkage of soil C-N-P stoichiometry to microbial resource limitation differed in karst and non-karst plantation forests in southwest China. *Catena* 231, 107341. <https://doi.org/10.1016/j.catena.2023.107341>.
- Yang, Y., Dou, Y., Wang, B., Xue, Z., et al., 2023b. Deciphering factors driving soil microbial life-history strategies in restored grasslands. *iMeta* 2, e66. <https://doi.org/10.1002/imt.2.66>.

- Yang, Y., Li, P., Ding, J., Zhao, X., et al., 2014. Increased topsoil carbon stock across China's forests. *Glob. Change Biol.* 20, 2687–2696. <https://doi.org/10.1111/gcb.12536>.
- Yang, Y., Gunina, A., Cheng, H., Liu, L., et al., 2025. Unlocking mechanisms for soil organic matter accumulation: carbon use efficiency and microbial necromass as the keys. *Glob. Change Biol.* 31, e70033. <https://doi.org/10.1111/gcb.70033>.
- Yu, J., Yang, J., Qu, L., Huang, X., et al., 2025. Soil microbial carbon use efficiency differs between mycorrhizal trees: insights from substrate stoichiometry and microbial networks. *ISME Communications* 5, ycae173. <https://doi.org/10.1093/ismeco/ycae173>.
- Yu, Z., Liu, S., Li, H., Liang, J., et al., 2024. Maximizing carbon sequestration potential in Chinese forests through optimal management. *Nat. Commun.* 15, 3154. <https://doi.org/10.1038/s41467-024-471435>.
- Yuan, N., Fang, F., Tang, X., Lv, S., et al., 2024. Degradation-driven vegetation-soil-microbe interactions alter microbial carbon use efficiency in Moso bamboo forests. *Sci. Total Environ.* 951, 175435. <https://doi.org/10.1016/j.scitotenv.2024.175435>.
- Yuan, X.B., Niu, D.C., Gherardi, L.A., Liu, Y.B., et al., 2019. Linkages of stoichiometric imbalances to soil microbial respiration with increasing nitrogen addition: evidence from a long-term grassland experiment. *Soil Biol. Biochem.* 138. <https://doi.org/10.1016/j.soilbio.2019.107580>.
- Zhang, G., Zhang, P., Peng, S., Chen, Y., Cao, Y., 2017. The coupling of leaf, litter, and soil nutrients in warm temperate forests in northwestern China. *Sci. Rep.* 7, 11754. <https://doi.org/10.1038/s41598-017-121995>.
- Zhang, Q., Wang, X., Zhang, Z., Liu, H., et al., 2022. Linking soil bacterial community assembly with the composition of organic carbon during forest succession. *Soil Biol. Biochem.* 173, 108790. <https://doi.org/10.1016/j.soilbio.2022.108790>.
- Zheng, H., Hedéne, P., Rousk, J., Schmidt, I.K., et al., 2022. Effects of common European tree species on soil microbial resource limitation, microbial communities and soil carbon. *Soil Biol. Biochem.* 172, 108754. <https://doi.org/10.1016/j.soilbio.2022.108754>.
- Zheng, Y., Ye, J., Pei, J., Fang, C., et al., 2024. Initial soil condition, stand age, and aridity alter the pathways for modifying the soil carbon under afforestation. *Sci. Total Environ.* 946, 174448. <https://doi.org/10.1016/j.scitotenv.2024.174448>.
- Zhong, Z., Li, W., Lu, X., Gu, Y., et al., 2020. Adaptive pathways of soil microorganisms to stoichiometric imbalances regulate microbial respiration following afforestation in the Loess Plateau, China. *Soil Biol. Biochem.* 151. <https://doi.org/10.1016/j.soilbio.2020.108048>.
- Zhou, J., Liu, Y., Liu, C., Zamanian, K., et al., 2024a. Necromass responses to warming: a faster microbial turnover in favor of soil carbon stabilisation. *Sci. Total Environ.* 954, 176651. <https://doi.org/10.1016/j.scitotenv.2024.176651>.
- Zhou, X., Chen, X., Yang, K., Guo, X., et al., 2024b. Vegetation restoration in an alpine meadow: insights from soil microbial communities and resource limitation across soil depth. *J. Environ. Manag.* 360, 121129. <https://doi.org/10.1016/j.jenvman.2024.121129>.
- Zhou, Z., Wang, C., Luo, Y., 2018. Effects of forest degradation on microbial communities and soil carbon cycling: a global meta-analysis. *Global Ecol. Biogeogr.* 27, 110–124. <https://doi.org/10.1111/geb.12663>.